

## Investigation of poly(o-anisidine)-SnO<sub>2</sub> nanocomposites for fabrication of low temperature operative liquefied petroleum gas sensor

Dewyani Patil, Kishor Kolhe, Hari S. Potdar, and Pradip Patil

Citation: *Journal of Applied Physics* **110**, 124501 (2011); doi: 10.1063/1.3667107

View online: <http://dx.doi.org/10.1063/1.3667107>

View Table of Contents: <http://scitation.aip.org/content/aip/journal/jap/110/12?ver=pdfcov>

Published by the [AIP Publishing](#)

---

### Articles you may be interested in

[Synthesis, characterization, and gas-sensing properties of monodispersed SnO<sub>2</sub> nanocubes](#)

*Appl. Phys. Lett.* **105**, 053102 (2014); 10.1063/1.4892166

[Dielectric properties of poly\(vinylidene fluoride\) nanocomposites filled with surface coated BaTiO<sub>3</sub> by SnO<sub>2</sub> nanodots](#)

*Appl. Phys. Lett.* **104**, 072906 (2014); 10.1063/1.4866269

[CdSe quantum dots-poly\(3-hexylthiophene\) nanocomposite sensors for selective chloroform vapor detection at room temperature](#)

*Appl. Phys. Lett.* **101**, 173108 (2012); 10.1063/1.4762861

[Role of SnO<sub>2</sub> as a filler in \(PEO\)<sub>50</sub>AgCF<sub>3</sub>SO<sub>3</sub> nanocomposite polymer electrolyte system](#)

*AIP Conf. Proc.* **1447**, 399 (2012); 10.1063/1.4710048

[Sn O<sub>2</sub> thick films for room temperature gas sensing applications](#)

*J. Appl. Phys.* **106**, 124509 (2009); 10.1063/1.3273323

---



**AIP** | Journal of Applied Physics

*Journal of Applied Physics* is pleased to announce **André Anders** as its new Editor-in-Chief

## Investigation of poly(o-anisidine)-SnO<sub>2</sub> nanocomposites for fabrication of low temperature operative liquefied petroleum gas sensor

Dewyani Patil,<sup>1</sup> Kishor Kolhe,<sup>2</sup> Hari S. Potdar,<sup>3</sup> and Pradip Patil<sup>1,a)</sup>

<sup>1</sup>Department of Physics, North Maharashtra University, Jalgaon 425 001, Maharashtra State, India

<sup>2</sup>Sardar Vallabhbhai Patel Arts and Science College, Ainpur 425 509, Dist.- Jalgaon, Maharashtra State, India

<sup>3</sup>Physical and Materials Chemistry Division, National Chemical Laboratory, Dr. Homi Bhabha Road, Maharashtra, Pune 411 008, India

(Received 15 July 2011; accepted 10 November 2011; published online 19 December 2011)

Poly(o-anisidine)-tin oxide (POA-SnO<sub>2</sub>) nanocomposites has been investigated for the fabrication of low temperature operative (100 °C) liquefied petroleum gas (LPG) sensor. The POA-SnO<sub>2</sub> nanocomposites have been synthesized through an *in situ* chemical polymerization of o-anisidine in presence of SnO<sub>2</sub> nanoparticles. The POA-SnO<sub>2</sub> nanocomposite shows better LPG sensing properties than that of pure POA. The nanocomposite with 50 wt. % SnO<sub>2</sub> exhibits an excellent LPG sensing characteristics at the operating temperature of 100 °C such as higher relative gas response (~23.47% to 3.4% of LPG), extremely rapid response (~6 s), fast recovery (~33 s), good reproducibility, and remarkable selectivity. The application of POA-SnO<sub>2</sub> nanocomposites for fabrication of the LPG sensor was demonstrated. © 2011 American Institute of Physics. [doi:10.1063/1.3667107]

### I. INTRODUCTION

Over the last decade, considerable attention has been focused on the development of suitable gas sensitive materials for the fabrication of low cost, selective and low temperature operative gas sensors.<sup>1–3</sup> Metal oxides<sup>4</sup> and conducting polymers<sup>5</sup> have been widely investigated as sensing materials for the fabrication of gas sensors. However, both of them have certain advantages and drawbacks. Though metal oxides, such as SnO<sub>2</sub>,<sup>6</sup> Fe<sub>2</sub>O<sub>3</sub>,<sup>7</sup> WO<sub>3</sub>,<sup>8</sup> and ZnO,<sup>9</sup> either in undoped or doped forms have emerged as economical sensors for monitoring toxic gases, the need for elevated operating temperatures increases power consumption, reduces sensor life and limits the portability. In particular, SnO<sub>2</sub> is extensively used in the fabrication of gas sensors for detecting various toxic and flammable gases.<sup>6,10–12</sup> In order to enhance the gas response and selectivity toward certain gases or to reduce the operating temperature, SnO<sub>2</sub> is commonly modified by a small amount of dopants or its particle size is reduced to the nanoscale (<10 nm).<sup>10,13,14</sup> However, the gas sensors based on SnO<sub>2</sub> are still operated at temperatures above 200 °C due to its high resistance.<sup>15</sup> Consequently, the development of low temperature operative SnO<sub>2</sub> based sensors with high gas response and low fabrication cost has attracted much attention.

Conducting polymers such as polyaniline (PANI),<sup>16</sup> polypyrrole (PPY)<sup>17</sup> and polythiophene (PTH)<sup>18</sup> are also being investigated for gas sensing applications, as they have distinct advantages of easy processing, low cost and room temperature operation. However, similar to the metal oxides, they also exhibit certain limitations such as a low gas response, irreversibility, long recovery time and lack of specificity.

Among several different strategies for fabricating selective and low temperature operative gas sensors, the combination of nanostructured metal oxides with conducting polymers has been particularly interesting. In recent years, conducting polymer-metal oxide composites have been synthesized and based on these composites gas sensors have also been developed by few research groups. Geng *et al.* synthesized PANI-SnO<sub>2</sub>,<sup>19</sup> PPY-WO<sub>3</sub>,<sup>20</sup> PPY-ZnO,<sup>21</sup> and PPY-γ-Fe<sub>2</sub>O<sub>3</sub>,<sup>22</sup> composites and investigated the gas sensing properties. Tai *et al.*<sup>23,24</sup> investigated the NH<sub>3</sub> and CO sensing properties of PANI-TiO<sub>2</sub> nanocomposite thin films. Ma *et al.*<sup>25</sup> also prepared the PANI-TiO<sub>2</sub> composite film by using a combination of *in situ* polymerization and sol-gel methods and examined the gas sensitivity to trimethylamine at room temperature. Ram *et al.*<sup>26</sup> studied the CO sensing properties of a self-assembled PANI-TiO<sub>2</sub> or PANI-SnO<sub>2</sub> ultrathin films. Suri *et al.*<sup>27</sup> studied the gas sensors (CO<sub>2</sub>, N<sub>2</sub> and CH<sub>4</sub>) based on PPY/α-Fe<sub>2</sub>O<sub>3</sub> nanocomposites. Apart from this, there are few scattered studies on the gas sensors based on other conducting polymer-metal oxide nanocomposites such as PPY-MoO<sub>3</sub>,<sup>28</sup> PANI-In<sub>2</sub>O<sub>3</sub>,<sup>29</sup> PPY-SnO<sub>2</sub>,<sup>30</sup> cobalt porphyrin-SnO<sub>2</sub>,<sup>31</sup> etc. were reported in the literature. However, to our knowledge, there is still no report about LPG sensing at low operating temperatures using conducting polymer-metal oxide nanocomposites.

LPG is widely used as fuel for domestic heating and industrially to provide a clean source of energy for burning.<sup>32</sup> It is potentially hazardous due to the high possibility of explosion accidents caused by leakage or by human error. This has stimulated considerable interest for scientific research to develop reliable, efficient, simple and cost-effective chemical sensors to monitor LPG having good sensitivity and selectivity in recent years and many efforts, in this field, are today devoted to the synthesis of novel sensing materials with enhanced performance.

<sup>a)</sup>Author to whom correspondence should be addressed. Electronic mail: pnmu@yahoo.co.in.

The present study reports, for the first time to the best of our knowledge, on LPG sensor featuring a POA-SnO<sub>2</sub> nanocomposite as the sensitive layer. In this study, the POA-SnO<sub>2</sub> nanocomposites were synthesized by using an *in situ* chemical polymerization route and their LPG sensing properties were investigated, particularly focusing on the low temperature detection (25–100 °C). The POA was chosen as an organic counterpart for this study to explore the possibility of utilizing it as an alternative to PANI for gas sensing application. The nanocomposite with 50 wt. % SnO<sub>2</sub> exhibits an excellent LPG sensing characteristics such as higher relative gas response, extremely rapid response, fast recovery, good reproducibility and remarkable selectivity. A sensing mechanism was also discussed based on experimental findings.

## II. EXPERIMENTAL

Analytical reagent grade chemicals and de-ionized water were used throughout the present study. The monomer o-anisidine was procured from Fluka and it was doubly distilled prior to being used for the synthesis. The tin oxide (SnO<sub>2</sub>), ammonium persulphate [(NH<sub>4</sub>)<sub>2</sub>S<sub>2</sub>O<sub>8</sub>] and hydrochloric acid (HCl) were purchased from E-Merck (India) and were used as-received.

In a typical experiment, SnO<sub>2</sub> nanoparticles (25–40 nm in diameters) were added to HCl (1 M) and sonicated for 2 h in order to keep them well dispersed and suspended in the solution. After sonication, o-anisidine was added to this dispersion of SnO<sub>2</sub>. The oxidant (NH<sub>4</sub>)<sub>2</sub>S<sub>2</sub>O<sub>8</sub> (0.1 M) was then slowly added drop wise to well dispersed reaction mixture with continuous stirring at 0–5 °C and the reaction was continued for another 24 h. The dark green colored suspension was then filtered and washed several times with de-ionized water and methanol, and dried at 80 °C under vacuum for 24 h. Different POA-SnO<sub>2</sub> nanocomposites were synthesized using 30, 50, and 70 wt. % of SnO<sub>2</sub> with respect to o-anisidine, which are referred as POA-SnO<sub>2</sub>-30, POA-SnO<sub>2</sub>-50, and POA-SnO<sub>2</sub>-70, respectively. For comparison, pure POA was also synthesized following the same procedure without SnO<sub>2</sub> nanoparticles. The transmission electron microscopy (TEM) was used to determine the morphology of the POA-SnO<sub>2</sub> nanocomposite with a JEOL (1200 EX, JEOL, Japan).

The POA-SnO<sub>2</sub> nanocomposite powder was pressed into pellet form of (diameter ~1 cm and thickness ~0.1 cm) and the electrical contact leads were fixed 0.7 cm apart with the help of silver paste on the surface of the pellet to form sensing element. The LPG sensing experiments were carried out in a static gas chamber in air ambient. The sensing element was kept directly on a heater in the chamber and temperature was varied from room temperature (25 °C) to 100 °C. The temperature of the sensing element was monitored by chromel-alumel thermocouple placed in contact with the sensor. The known volume of the LPG was introduced into the gas chamber prefilled with air and it was maintained at atmospheric pressure. The dc current signal was measured as a function of time at a constant applied voltage of 1 V using an electrochemical measurement System (1287, Solartron,

UK) controlled by CorrWare software from Scribner Associates Inc. supplied by Solartron, UK. The resistance as a function of time was calculated from this data. The performance of the sensing element is presented in terms of gas response (S), which is defined by the relation:

$$S = \frac{R_g - R_a}{R_a} \times 100\%, \quad (1)$$

where  $R_a$  and  $R_g$  are values of the resistance in air and in presence of LPG, respectively.

## III. RESULTS AND DISCUSSION

More recently, we have synthesized the POA-SnO<sub>2</sub> nanocomposites by using an *in situ* chemical polymerization route and investigated humidity sensing properties.<sup>33</sup> The polymerization of o-anisidine has been successfully achieved on the surface of the SnO<sub>2</sub> nanoparticles as revealed by XRD and FTIR studies. In this study, the POA-SnO<sub>2</sub> nanocomposites were synthesized by using same procedure as reported earlier<sup>33</sup> and their LPG sensing properties were investigated, particularly focusing on the low temperature detection (25–100 °C).

### A. TEM analysis

The TEM image of the SnO<sub>2</sub> nanoparticles is shown in Fig. 1(a). It indicates the presence of SnO<sub>2</sub> nanoparticles with clear boundaries and crystal line with an average size of ~25–30 nm. The HRTEM image [Fig. 1(b)] shows well developed lattice fringes, which are in agreement with the XRD result (not shown here). The selected area electron diffraction (SAED) pattern [inset of Fig. 1(a)] shows a spot type pattern indicative of polycrystalline nature of the SnO<sub>2</sub> and no evidence was found for more than one pattern, suggesting the single phase nature of the material. The TEM image of the POA-SnO<sub>2</sub>-30 nanocomposite shown in Fig. 1(c) indicates the presence of dark colored SnO<sub>2</sub> nanoparticles are wrapped and interconnected with POA in the nanocomposite. It is observed that the SnO<sub>2</sub> nanoparticles are homogeneously distributed in the nanocomposite. The HRTEM image [Fig. 1(d)] indicates well developed lattice fringes and the SAED pattern of POA-SnO<sub>2</sub>-30 nanocomposite [inset of Fig. 1(c)] shows the diffraction rings composed of spots corresponding to the different planes of the tetragonal SnO<sub>2</sub>, which is in agreement with the XRD result (not shown here).

### B. LPG sensing characteristics

The LPG sensing experiments were performed at different temperatures in the range between room temperature (25 °C) and 100 °C in order to find out the optimum operating temperature for LPG detection. Before exposing to the LPG, the sensing element was allowed to equilibrate inside the gas chamber at an operating temperature for 1 h. A number of experiments have been carried out to measure the gas response as a function of the operating temperature. All the time the gas response of the sensor element has approximately constant values, indicating the repeatability of the

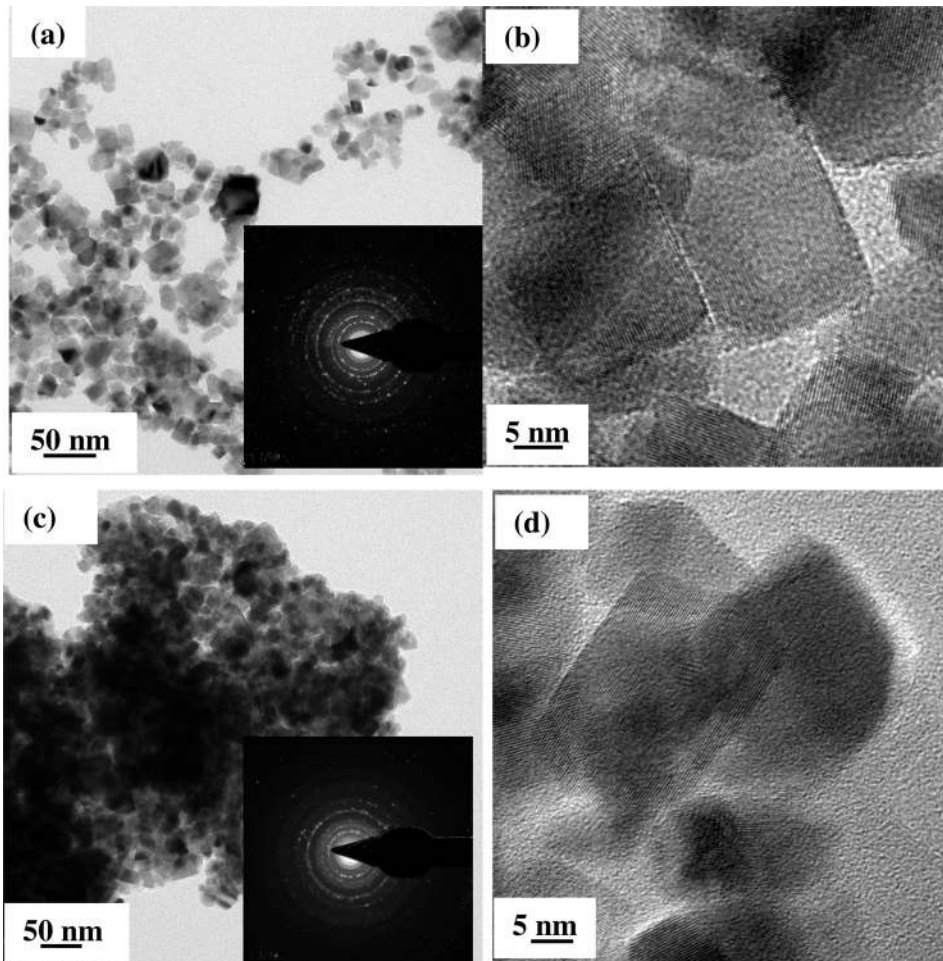


FIG. 1. TEM and HRTEM images of  $\text{SnO}_2$  nanoparticles (a,b) and POA- $\text{SnO}_2$ -30 nanocomposite (c,d). The corresponding SAED patterns are shown inset of (a) and (c).

sensor. The gas response of  $\text{SnO}_2$  nanoparticles, pure POA and POA- $\text{SnO}_2$  nanocomposites to 3.4% LPG as a function of operating temperature is shown in Fig. 2.  $\text{SnO}_2$  nanoparticles [Fig. 2(a)] did not show any response (i.e., no change in pellet resistance upon exposure to LPG) to LPG at operat-

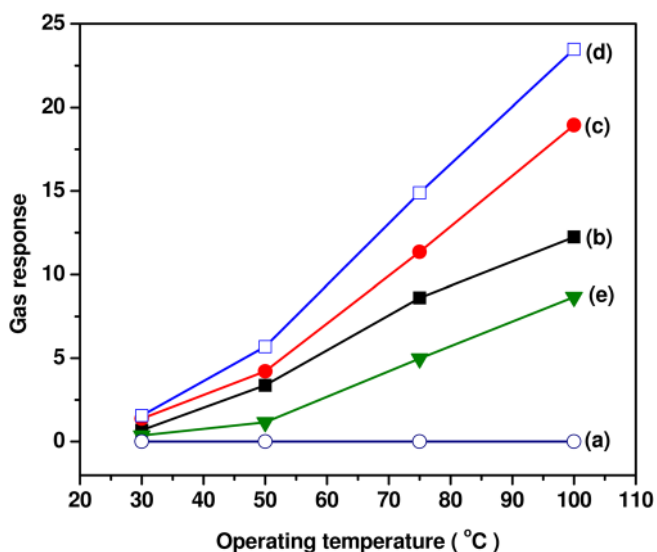


FIG. 2. (Color online) Response of (a)  $\text{SnO}_2$  nanoparticles, (b) pure POA and nanocomposites (c) POA- $\text{SnO}_2$ -30, (d) POA- $\text{SnO}_2$ -50, and (e) POA- $\text{SnO}_2$ -70 to 3.4% LPG as a function of operating temperature.

ing temperatures in the range between 25 and 100 °C. By contrast, pure POA is found to be sensitive to LPG [Fig. 2(b)] at operating temperatures in the range between 25 and 100 °C and it exhibits relative response of  $\sim 0.67\%$  to 3.4% LPG at 25 °C. Furthermore, its relative LPG response increases with an increase in the operating temperature and it is maximum ( $\sim 12.24\%$ ) at the operating temperature of 100 °C.

Interestingly, the POA- $\text{SnO}_2$  nanocomposites are reversibly responded to LPG even at room temperature and with increasing sensing temperature, the magnitude of relative LPG response increases. It is observed that the relative LPG responses of POA- $\text{SnO}_2$  nanocomposites (with 30 and 50 wt. % of  $\text{SnO}_2$ ) are much higher than that of pure POA irrespective of the operating temperatures. The relative LPG response is the maximum for the nanocomposite with 50 wt. % of  $\text{SnO}_2$  and it decreases on further increasing or decreasing the concentration of  $\text{SnO}_2$  in the nanocomposite. The POA- $\text{SnO}_2$ -50 nanocomposite exhibits maximum relative LPG response of  $\sim 23.47\%$  to 3.4% LPG at the operating temperature of 100 °C, which is 1.92 times higher than that of pure POA.

The POA- $\text{SnO}_2$ -50 nanocomposite showing maximum LPG response was chosen for further study to evaluate the response and recovery times, reproducibility and selectivity. In order to investigate the reproducibility and reversibility, the POA and POA- $\text{SnO}_2$ -50 nanocomposite were repeatedly

exposed to 3.4% LPG at the operating temperature of 25 °C. Figure 3 represents the relative LPG responses of pure POA and POA-SnO<sub>2</sub>-50 nanocomposite upon periodic exposure to 3.4% LPG at the operating temperature of 25 °C. As can be seen from Fig. 3(a), the resistance of pure POA rapidly increases upon exposure to LPG but it fails to return to the initial value after removal of the gas. Thus, the POA indicates the poor reversibility to LPG and its maximum relative LPG response to 3.4% LPG at 25 °C is found to be ~0.67%.

When the POA-SnO<sub>2</sub>-50 nanocomposite is exposed to LPG [Fig. 3(b)] at 25 °C, a rapid increase in the resistance is observed. After the removal of the LPG, the resistance of the nanocomposite was observed to recover slowly due to desorption of LPG molecules from nanocomposite. The relative LPG response of POA-SnO<sub>2</sub>-50 nanocomposite to 3.4% LPG at room temperature is found to be ~1.55%, which is 2.31 times higher than pure POA. The repeated tests reveals that the relative LPG response values are maintained and the recovery abilities are not reduced after several sensing cycles. Such behavior indicates that the POA-SnO<sub>2</sub>-50 nanocomposite based sensor has a stable and repeatable characteristic at 25 °C. Thus, the POA-SnO<sub>2</sub>-50 nanocomposite can be reversibly used for the detection of LPG at 25 °C.

Besides the gas response, the response and recovery times are also important for evaluating the performance of gas sensors. The time taken by a sensor to achieve 90% of the total resistance change is defined as response time in the case of adsorption or the recovery time in the case of desorption. The response and recovery characteristics of pure POA and POA-SnO<sub>2</sub>-50 nanocomposite to 3.4% LPG at the operating temperature of 25 °C are shown in Fig. 4. As can be seen from Fig. 4(a), pure POA responds rapidly after introduction of LPG, however it does not recover when it is exposed to air. Pure POA has response time of ~5–7 s at 25 °C. A considerable enhancement in rate of response is observed for POA-SnO<sub>2</sub>-50 nanocomposite [Fig. 4(b)] at room temperature. It is observed that the resistance of the POA-SnO<sub>2</sub>-50 nanocomposite very rapidly increases when exposed to the LPG and recovers immediately when it is exposed to air. The POA-SnO<sub>2</sub>-50 nanocomposite has

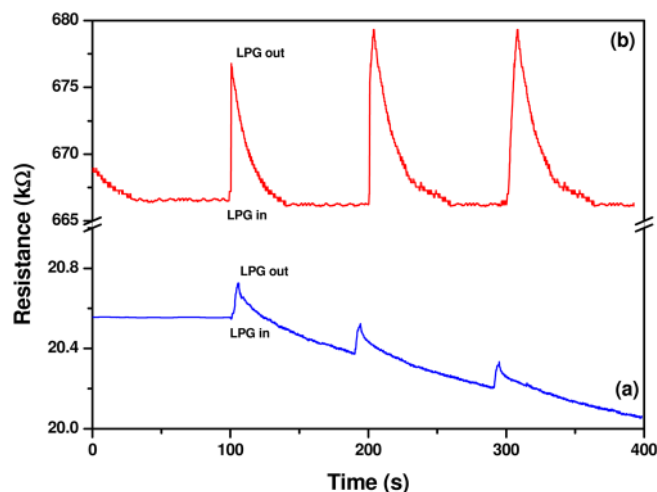


FIG. 3. (Color online) Repetitive response of (a) pure POA and (b) POA-SnO<sub>2</sub>-50 nanocomposite to 3.4% LPG at the operating temperature of 25 °C.

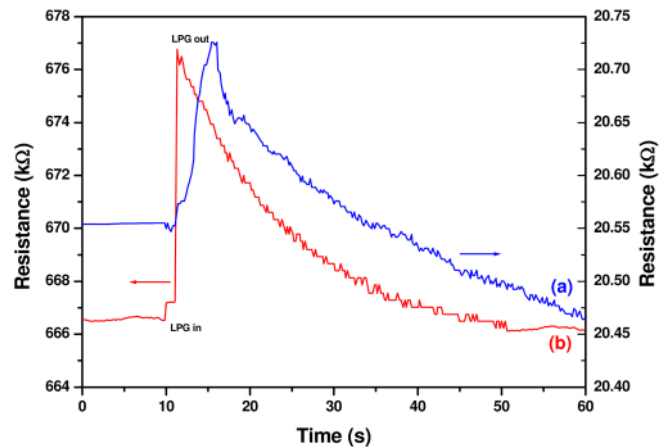


FIG. 4. (Color online) Response of (a) pure POA and (b) POA-SnO<sub>2</sub>-50 nanocomposite to 3.4% LPG at the operating temperature of 25 °C.

response and recovery times ~3–5 s and the recovery time of ~40 s at 25 °C. This clearly indicates that the POA-SnO<sub>2</sub>-50 nanocomposite is more sensitive to LPG at 25 °C than pure POA. The distinct response to LPG under the identical experimental conditions is attributed to the different degree of interactions between the adsorbed LPG and the different sensing materials that is POA and POA-SnO<sub>2</sub>-50 nanocomposite.

The relative LPG responses of pure POA and POA-SnO<sub>2</sub>-50 nanocomposite upon periodic exposure to 3.4% LPG at the operating temperature of 100 °C are shown in Fig. 5. A comparison of the results from measurements at 25 and 100 °C suggests that the gas response for pure POA as well as for POA-SnO<sub>2</sub>-50 nanocomposite is observed to increase at the operating temperature of 100 °C. The maximum relative LPG response of POA-SnO<sub>2</sub>-50 nanocomposite to 3.4% LPG is found to be ~23.47, which is 1.92 times higher than that of pure POA. The relative LPG response of POA-SnO<sub>2</sub>-50 nanocomposite is almost reproducible and stable. Furthermore, no significant variation in the relative

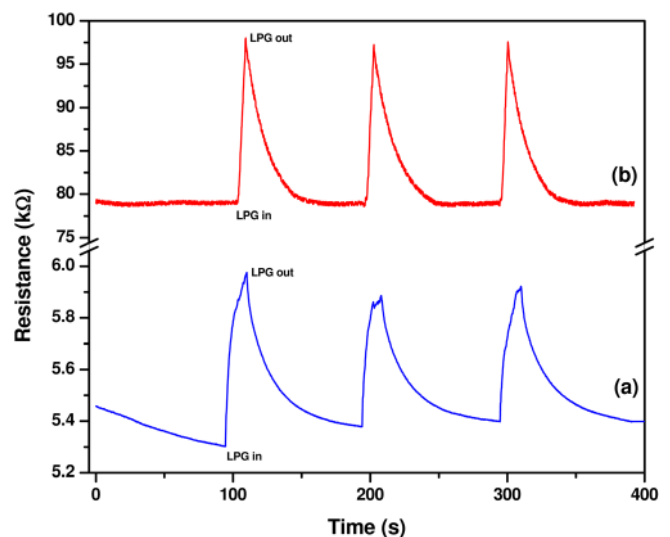


FIG. 5. (Color online) Repetitive response of (a) pure POA and (b) POA-SnO<sub>2</sub>-50 nanocomposite to 3.4% LPG at the operating temperature of 100 °C.

LPG response values is observed during the test for more than three times as shown in Fig. 5(b).

The response and recovery characteristics of pure POA and POA-SnO<sub>2</sub>-50 nanocomposite to 3.4% LPG at the operating temperature of 100 °C are shown in Fig. 6. Pure POA exhibits a response time of about 10–12 s at 100 °C, which decreased to about 5–6 s for the POA-SnO<sub>2</sub>-50 nanocomposite. A decrease in the recovery time is also observed for the POA-SnO<sub>2</sub>-50 nanocomposite and it is found to be ~33 s. Thus, the POA-SnO<sub>2</sub>-50 nanocomposite exhibits a very fast response (~5–6 s) and rapid recovery (~33 s) for LPG at the operating temperature of 100 °C. Thus, the optimum operating temperature of 100 °C is chosen in order to investigate further the LPG sensing properties of the POA-SnO<sub>2</sub>-50 nanocomposite.

Figure 7 represents the relative LPG response of POA-SnO<sub>2</sub>-50 nanocomposite at the operating temperature of 100 °C to LPG with concentrations varying from 0.07 to 4%. It is observed that the relative LPG response increases with an increase of the LPG concentration. Furthermore, a baseline remains stable and it has good reversibility. The dependence of the relative LPG response of the POA-SnO<sub>2</sub>-50 nanocomposite on the LPG concentration at the operating temperature 100 °C is shown in Fig. 8. The relative LPG response changed from 0.80% to 23.64% in the investigated range of 0.07 to 4%. The POA-SnO<sub>2</sub>-50 nanocomposite is able to detect up to 0.07% for LPG with reasonable relative LPG response (~0.80%) at 100 °C. It is observed that the relative LPG response increases linearly as the LPG concentration increases from 0.14 to 4% and then it saturates with further increase in the LPG concentration. It is found that the response of POA-SnO<sub>2</sub>-50 nanocomposite can be empirically represented as  $y = 0.56 + 6.64 * x$ ,  $R = 0.9947$  where  $x$ ,  $y$ , and  $R$  represents the LPG concentration, gas response and correlation coefficient, respectively.) The dashed line shows the linear fit to the experimental data, which suggests that the POA-SnO<sub>2</sub>-50 nanocomposite can be reliably used to monitor the concentration of LPG over this range.

In order to examine the cross sensitivity of POA-SnO<sub>2</sub> nanocomposite based sensor to different gases and thereby to

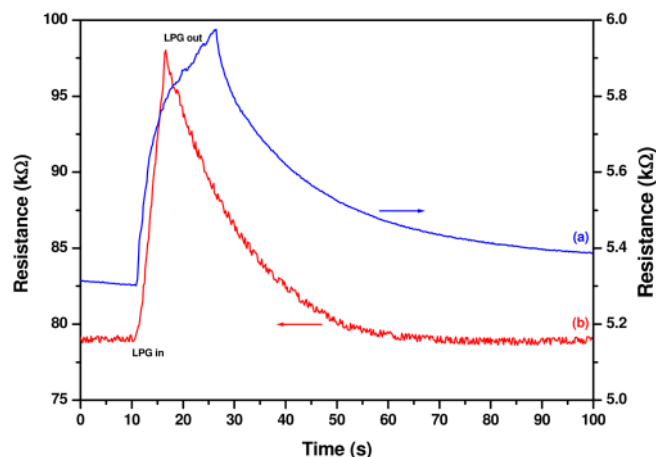


FIG. 6. (Color online) Response of (a) pure POA and (b) POA-SnO<sub>2</sub>-50 nanocomposite to 3.4% LPG at the operating temperature of 100 °C.

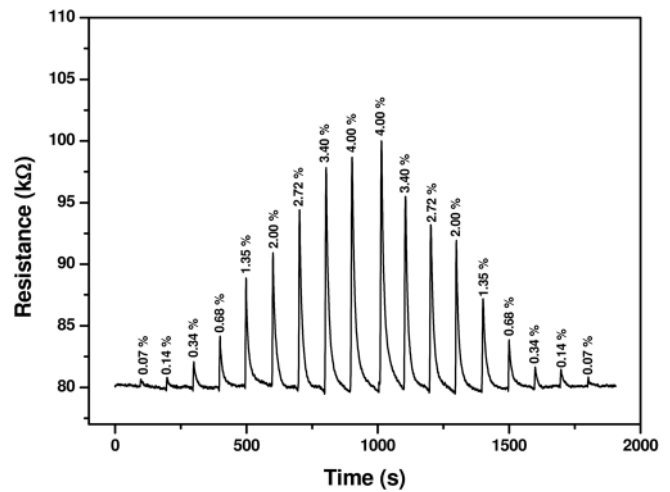


FIG. 7. Response of POA-SnO<sub>2</sub>-50 nanocomposite upon sequential exposure to LPG with concentrations varying from 0.07 to 4% at the operating temperature of 100 °C.

determine its selectivity to any particular gas, the behavior of pure POA and POA-SnO<sub>2</sub>-50 nanocomposite at an operating temperature of 100 °C under different gases was studied and the corresponding results are shown in Fig. 9. The gas response was monitored in the presence of H<sub>2</sub>, CO, CO<sub>2</sub>, and ethanol with concentration 3.4% each in addition to LPG. It can be seen that there is a distinct difference in gas responses of POA and POA-SnO<sub>2</sub>-50 nanocomposite to the tested gases. Pure POA shows almost nearly equal response values to H<sub>2</sub>, CO, CO<sub>2</sub>, and ethanol. On the other hand, the POA-SnO<sub>2</sub>-50 nanocomposite exhibits highest response for LPG and the least for H<sub>2</sub>. In order to quantify the selectivity to LPG, the selectivity coefficient ( $K$ ) was calculated further according to definition<sup>34</sup>

$$K = \frac{S_{\text{LPG}}}{S_B}, \quad (2)$$

where  $S_{\text{LPG}}$  and  $S_B$  are the responses of sensors in LPG and  $B$  gas, respectively. The selectivity coefficients for pure POA

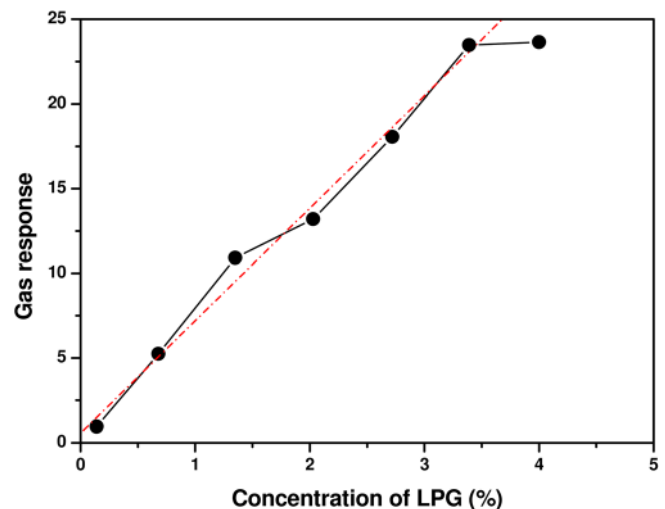


FIG. 8. (Color online) Relationship between gas response of POA-SnO<sub>2</sub>-50 nanocomposite and LPG concentration.

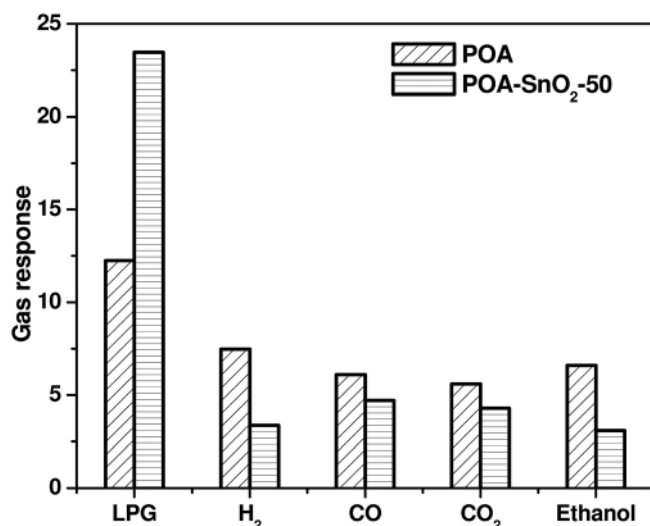


FIG. 9. Bar chart showing the gas response of pure POA and POA-SnO<sub>2</sub>-50 nanocomposite for different gases. The gas concentration and operating temperature in all cases were 3.4% and 100 °C, respectively.

were found to be 1.67 to H<sub>2</sub>, 2.05 to CO, 2.23 to CO<sub>2</sub>, 1.90 to ethanol, indicating the lack of selectivity to the tested gases. The preferentially high response exhibited by the POA-SnO<sub>2</sub>-50 nanocomposite toward LPG (23.47% to 3.4% LPG at 100 °C) compared to only 3.09–4.71% response in case of other gases like H<sub>2</sub>, CO, CO<sub>2</sub>, and ethanol is remarkable. The selectivity coefficient,  $K$  for the POA-SnO<sub>2</sub> nanocomposite varies in the order ethanol > H<sub>2</sub> > CO<sub>2</sub> > CO. This means that the fabricated sensor based on POA-SnO<sub>2</sub> nanocomposite could be used for the selective detection of LPG when there is a mixture of LPG and CO. Based on the observed results, it can be concluded that the formation of a composite of POA with SnO<sub>2</sub> nanoparticles is not only effective in enhancing the gas response but also in making it selective for the detection of LPG.

The experiments were also performed to investigate the influence of humidity on the relative LPG responses of pure POA and POA-SnO<sub>2</sub>-50 nanocomposite to 3.4% LPG at the operating temperature of 100 °C. In these experiments, the different relative humidity (RH) levels  $11 \pm 0.30$ ,  $33 \pm 0.14$ ,  $43 \pm 0.20$ ,  $75 \pm 0.15$ ,  $85 \pm 0.24$ , and  $97 \pm 0.16\%$  RH were generated in a simple gas sensing setup fabricated in our laboratory in order to investigate the effect of humidity on the relative LPG responses of pure POA and POA-SnO<sub>2</sub>-50 nanocomposite. It is seen that the LPG responses of pure POA and POA-SnO<sub>2</sub>-50 nanocomposite increases slowly in the humidity range 11–43% (not shown here) and thereafter, no significant change in the responses was observed with a further increase in RH.

### C. Comparison with other sensors

Before this study, few research groups have also investigated NH<sub>3</sub>, NO<sub>x</sub>, acetone and methanol gas sensing properties of conducting polymer-SnO<sub>2</sub> composites. However, there is still no report about LPG sensing at low operating temperatures using conducting polymer-SnO<sub>2</sub> composites. Mostly,

the conducting polymers PANI, PPY, and PTP were chosen as organic counter parts to synthesize various conducting polymer-SnO<sub>2</sub> composites. We have chosen the POA as organic counterpart in the present study to explore the possibility of utilizing them as an alternative to PANI for gas sensing application.

As mentioned earlier, hydrothermally synthesized PANI-SnO<sub>2</sub> hybrid was observed to be sensitive to ethanol and acetone at 60 or 90 °C with good reversibility.<sup>19</sup> The response time to ethanol and acetone was within 23–43 and 16–20 s, respectively, at 90 °C and the recovery time was within 16–28 and 35–48 s, respectively. However, the ethanol and acetone sensing properties of pure PANI have not been investigated and compared with those of the PANI-SnO<sub>2</sub> hybrid. Deshpande *et al.*<sup>35</sup> have synthesized the SnO<sub>2</sub>-intercalated PANI nanocomposite, which showed better sensitivity to ammonia gas at room temperature than SnO<sub>2</sub> with the response and recovery times of 12–15 s and 80 s for 300 ppm ammonia gas, respectively. However, pure PANI exhibited better sensitivity to ammonia than SnO<sub>2</sub>-intercalated PANI nanocomposite with relatively fast response (8–10 s) and slow recovery (160 s). Zhang *et al.*<sup>36</sup> studied ammonia sensor based on PPY-coated SnO<sub>2</sub> hollow spheres, which showed better response at room temperature than SnO<sub>2</sub> and pure PPY with the fast response (~9 s) and slow recovery (several minute). Xu *et al.*<sup>37</sup> reported the NO<sub>2</sub> sensor based on PTP-coated SnO<sub>2</sub> hollow spheres, which exhibited higher gas response and shorter recovery time for detecting NO<sub>2</sub> of ppm levels at 90 °C than the sensor based on pure PTP. Kong *et al.*<sup>38</sup> recently reported the synthesis of SnO<sub>2</sub>-PTP composites and studied their NO<sub>2</sub> sensing properties at low operating temperatures, which are better than SnO<sub>2</sub>. However, the NO<sub>2</sub> sensing properties of the pure PTP have not been investigated and compared with those of the SnO<sub>2</sub>-PTP composites. But the present LPG sensor based on POA-SnO<sub>2</sub> nanocomposites has a relative LPG response of 1.55% and 23.47% for 3.4% LPG at 25 and 100 °C, respectively, as shown in Figs. 3 and 5. Furthermore, it has a high response of 0.95–23.47% to 0.14–4% LPG (cf. Fig. 8), very fast response (~5–6 s), faster recovery (~33 s), excellent repeatability (cf. Fig. 7) and good selectivity (cf. Fig. 9) when operating at 100 °C. It is able to detect up to 0.07% LPG with reasonable gas response (~0.80) at 100 °C.

The POA-SnO<sub>2</sub> nanocomposites also have better LPG sensing characteristics than the semiconducting metal oxide based LPG sensors reported in the literature. Jiao *et al.*<sup>39</sup> reported the LPG sensor based on ZnGa<sub>2</sub>O<sub>4</sub> nanocrystals (10–20 nm) having a maximum sensitivity of ~7 at 410 °C and having response time of a few seconds, with a recovery time of ~60 s for 500 ppm LPG. Waghulade *et al.*<sup>40</sup> reported the synthesis of CdO nanoparticles by using chemical coprecipitation method and investigated their LPG sensing performance. The CdO nanoparticles showed a maximum sensitivity of 3.41 at 450 °C with the response and recovery times of 3–5 and 8–10 s for 25 ppm LPG, respectively. Salunke *et al.*<sup>41</sup> reported a chemical bath deposition of unsensitized and Pd-sensitized CdO nanorods and investigated their LPG sensing performance. The unsensitized CdO nanorods exhibited a maximum response of ~0.14 at 425 °C for

0.1 vol. % of LPG, which improved up to 0.35 at an optimum temperature of 375 °C after Pd-sensitization, with response and recovery times of 30 and 90 s, respectively. Phani *et al.*<sup>32</sup> investigated the LPG sensing property of Pd doped SnO<sub>2</sub>. The Pd (1.5 wt. %) doped SnO<sub>2</sub> showed a maximum sensitivity of 0.97 at 350 °C for 1000 ppm. Sahay *et al.*<sup>42</sup> reported a chemical spray deposited Al doped ZnO thin films used for LPG sensors. The 0.5 at. % Al doped ZnO thin films showed a maximum sensitivity of 0.89 at 325 °C for 1 vol. % of LPG. Chaudhari *et al.*<sup>43</sup> studied the LPG sensor based on nanosized BaTiO<sub>3</sub> (~65 nm) thick films, which showed a maximum sensitivity of 0.45 at 300 °C for 5000 ppm LPG and an improvement in the sensitivity and selectivity was observed by doping the BaTiO<sub>3</sub> with CuO and CdO. The LPG sensor based on POA-SnO<sub>2</sub> nanocomposite in this work has a reproducible and stable response to LPG even at room temperature. It is more sensitive to LPG than that of pure POA when operated at 25 or 100 °C. In short, the POA-SnO<sub>2</sub> nanocomposites can overcome the shortcomings of lower gas response, long response time, slow recovery and lack of selectivity of POA and higher operating temperature of SnO<sub>2</sub>, thus presenting very promising sensing material for the fabrication of LPG sensors operating at low temperatures.

#### D. LPG sensing mechanism

The experimental results presented so far can be interpreted in relation to the possible LPG sensing mechanism of the POA-SnO<sub>2</sub> nanocomposite. As already noted, pure POA is a *p*-type semiconductor and it is sensitive to LPG at low operating temperatures (25–100 °C). The adsorption of LPG at POA surface donates electrons and consequently its resistance increases. On the other hand, SnO<sub>2</sub> is an *n*-type semiconductor and the sensors based on SnO<sub>2</sub> are usually operated at temperatures above 200 °C due to its high resistance. The resistance of SnO<sub>2</sub> decreases, when exposed to the reducing gas LPG. The POA-SnO<sub>2</sub> nanocomposite is sensitive to LPG at low operating temperatures (25–100 °C) and when exposed to LPG, it exhibits the properties of *p*-type

semiconductor, that is, its resistance increases on exposure to LPG. This observation suggests that the LPG sensing mechanism of the nanocomposite is governed by POA, which is supported by TEM study. As revealed by TEM study, the SnO<sub>2</sub> nanoparticles are enwrapped and interconnected with POA in the nanocomposite and therefore, the active sites on the POA backbone are largely accessible to LPG. The relative gas response of nanocomposite toward LPG is noticeably higher than that of pure POA and SnO<sub>2</sub> nanoparticles individually due to its loose and porous structure. The nanocomposite exhibits excellent LPG sensing characteristics than pure POA, suggesting that the SnO<sub>2</sub> nanoparticles in the nanocomposite are also playing active role in the sensing process. In order to explain the gas sensing mechanism of conducting polymer/metal oxide nanocomposites, several researchers have postulated that conducting polymer and metal oxide may form a *p*–*n* junction and the observed sensing response of nanocomposite material may be due to the creation of a positively charged depletion layer on the surface of metal oxide.<sup>36–38</sup> The schematic representation of the model based on the principle of formation of heterojunction barrier is depicted in Fig. 10, to explain the LPG sensing behavior of POA-SnO<sub>2</sub> nanocomposite. When the nanocomposite is exposed to the LPG, the LPG gas molecules are adsorbed preferentially on POA and it leads to the interaction of LPG at the interface of *p*-POA/*n*-SnO<sub>2</sub> heterojunction. The adsorption of LPG at POA surface donates electrons and results in more negative acceptor ions in the *p*-side and hence a wider space charge layer. As the surface of SnO<sub>2</sub> nanoparticles is generally covered with negatively charged adsorbed O<sup>-</sup> ions, an electron depletion layer is created on *n*-side of the junction. As a result, the carrier concentration of the heterojunction decreases and consequently, the potential barrier height of the heterojunction increases and an increase in the resistance of the nanocomposite is observed. It can be said that in the POA-SnO<sub>2</sub> nanocomposite, POA identify LPG (receptor function) and both POA and SnO<sub>2</sub> nanoparticles provide conducting path (transducer function) and their nanocomposite permits selective detection of LPG at low operating temperatures (25–100 °C).

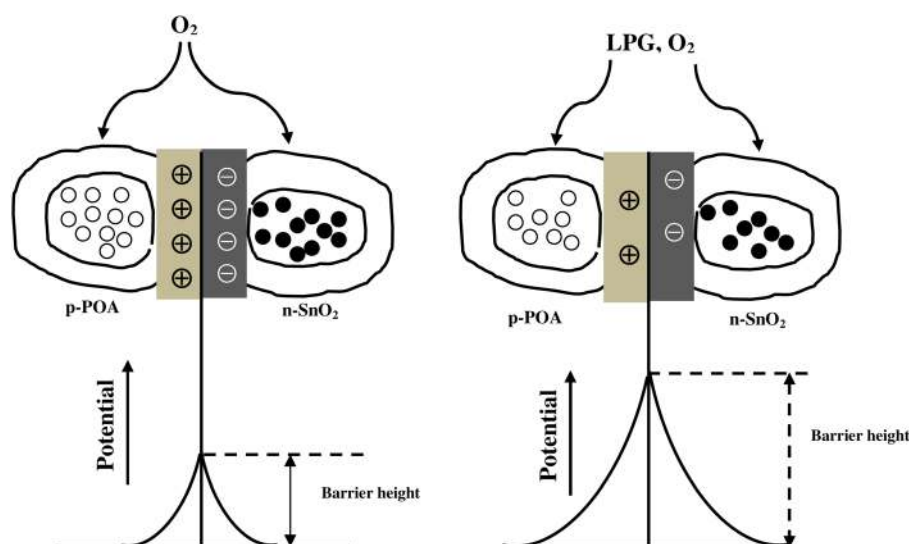


FIG. 10. (Color online) Schematic representation of LPG sensing model for POA-SnO<sub>2</sub> nanocomposite.



#### IV. CONCLUSIONS

This work reports the sensing characteristics of POA-SnO<sub>2</sub> nanocomposite toward LPG. The POA-SnO<sub>2</sub> nanocomposite overcomes the shortcomings of lower gas response, long response time, slow recovery and lack of selectivity of pure POA and higher operating temperature of SnO<sub>2</sub>. The LPG sensor based on POA-SnO<sub>2</sub> nanocomposite has a reproducible and stable response to LPG even at room temperature. It was shown that the POA-SnO<sub>2</sub>-50 nanocomposite is able to detect up to 0.07% LPG with reasonable gas response at 100 °C and it can be reliably used to monitor the concentration of LPG over the range (0.07–4%). Furthermore, it has a high response of 0.95–23.47% to 0.14–4% LPG, very fast response (~5–6 s), faster recovery (~33 s), excellent repeatability and good selectivity when operating at 100 °C. Thus, it was demonstrated that the POA-SnO<sub>2</sub> nanocomposite can be used as selective and reusable gas sensing material for the fabrication of LPG sensors operating at low temperatures.

#### ACKNOWLEDGMENTS

The financial support from University Grants Commission (UGC), New Delhi, India through the major research project No. F 34-3/2008 (SR) is gratefully acknowledged.

<sup>1</sup>E. Comini, *Anal. Chim. Acta* **568**, 28 (2006).

<sup>2</sup>C. Wang, X. Q. Fu, X. Y. Xue, Y. G. Wang, and T. H. Wang, *Nanotechnology* **18**, 145506 (2007).

<sup>3</sup>F. Zhang, A. Zhu, Y. Luo, Y. Tian, J. Yang, and Y. Qin, *J. Phys. Chem. C* **114**, 19214 (2010).

<sup>4</sup>G. F. Fine, L. M. Cavanagh, A. Afonja, and R. Binions, *Sensors* **10**, 5469 (2010).

<sup>5</sup>H. Bai and G. Shi, *Sensors* **7**, 267 (2007).

<sup>6</sup>A. Srivastava, K. Jain, Rashmi, A. K. Srivastava, and S. T. Lakshmikumar, *Mater. Chem. Phys.* **97**, 85 (2006).

<sup>7</sup>D. Patil, V. Patil, and P. Patil, *Sens. Actuators B* **152**, 299 (2011).

<sup>8</sup>R. S. Khadayate, J. V. Sali, and P. P. Patil, *Talanta* **72**, 1077 (2007).

<sup>9</sup>J. Kim and K. Yong, *J. Phys. Chem. C* **115**, 7218 (2011).

<sup>10</sup>R. S. Niranjana, Y. K. Hwang, D. K. Kim, S. H. Jung, J. S. Chang, and I. S. Mulla, *Mater. Chem. Phys.* **92**, 384 (2005).

<sup>11</sup>G. J. Li and S. Kawi, *Talanta* **59**, 667 (2003).

<sup>12</sup>A. Chowdhari, V. Gupta, K. Sreenivas, R. Kumar, S. Mozumdar, and P. K. Patanjali, *Appl. Phys. Lett.* **84**, 1180 (2004).

<sup>13</sup>N. Yamazoe, *Sens. Actuators B* **5**, 7 (1991).

<sup>14</sup>D. Kohl, *Sens. Actuators B* **1**, 158 (1990).

<sup>15</sup>S. Seal and S. Shukla, *JOM* **54**, 35 (2002).

<sup>16</sup>H. Liu, J. Kameoka, D. A. Czaplewski, and H. G. Craighead, *Nano Lett.* **4**, 671 (2004).

<sup>17</sup>Q. Fang, D. G. Chetwynd, J. A. Covington, C. S. Toh, and J. W. Gardner, *Sens. Actuators B* **84**, 66 (2002).

<sup>18</sup>R. Rella, P. Siciliano, F. Quaranta, T. Primo, L. Valli, L. Schenetti, A. Mucci, and D. Iarossi, *Sens. Actuators B* **68**, 203 (2000).

<sup>19</sup>L. Geng, Y. Zhao, X. Huang, S. Wang, S. Zhang, and S. Wu, *Sens. Actuators B* **120**, 568 (2007).

<sup>20</sup>L. Geng, X. Huang, Y. Zhao, P. Li, S. Wang, S. Zhang, and S. Wu, *Solid-State Electron.* **50**, 723 (2006).

<sup>21</sup>L. Geng, Y. Zhao, X. Huang, S. Wang, S. Zhang, W. Huang, and S. Wu, *Synth. Met.* **156**, 1078 (2006).

<sup>22</sup>L. Geng, S. Wang, Y. Zhao, P. Li, S. Zhang, W. Huang, and S. Wu, *Mater. Chem. Phys.* **99**, 15 (2006).

<sup>23</sup>H. Tai, Y. Jiang, G. Xie, J. Yu, and X. Chen, *Sens. Actuators B* **125**, 644 (2007).

<sup>24</sup>H. Tai, Y. Jiang, G. Xie, J. Yu, X. Chen, and Z. Ying, *Sens. Actuators B* **129**, 319 (2008).

<sup>25</sup>X. Ma, M. Wang, G. Li, H. Chena, and R. Baia, *Mater. Chem. Phys.* **99**, 15 (2006).

<sup>26</sup>M. K. Ram, O. Yavuz, V. Lahsangah, and M. Aldissi, *Sens. Actuators B* **106**, 750 (2005).

<sup>27</sup>K. Suri, S. Annapoorni, A. K. Sarkar, and R. P. Tandon, *Sens. Actuators B* **81**, 277 (2002).

<sup>28</sup>K. Hosono, I. Matsubara, N. Murayama, S. Woosuck, and N. Izu, *Chem. Mater.* **17**, 349 (2005).

<sup>29</sup>A. Z. Sadek, W. Wlodarski, K. Shin, R. Bkaner, and K. Kalantar-zadeh, *Nanotechnology* **17**, 4488 (2006).

<sup>30</sup>P. J. Benjamin, E. Phillip, J. E. Richard, L. H. Colin, and M. R. Norman, *J. Mater. Chem.* **6**, 289 (1996).

<sup>31</sup>S. Nardis, D. Monti, C. D. Natable, A. D. Amico, P. Siciliano, A. Forleo, M. Epifani, A. Taurino, R. Rella, and R. Paolesse, *Sens. Actuators B* **103**, 339 (2004).

<sup>32</sup>A. R. Phani, *Appl. Phys. Lett.* **71**, 2358 (1997).

<sup>33</sup>D. Patil, Y. K. Seo, Y. K. Hwang, and P. Patil, *Sens. Actuators B* **148**, 41 (2010).

<sup>34</sup>M. Siemons and U. Simon, *Sens. Actuators B* **126**, 595 (2007).

<sup>35</sup>N. G. Deshpande, Y. G. Gudagea, R. Sharma, J. C. Vyas, J. B. Kim, and Y. P. Lee, *Sens. Actuators B* **138**, 76 (2009).

<sup>36</sup>J. Zhang, S. Wang, M. Xu, Y. Wang, H. Xia, S. Zhang, X. Guo, and S. Wu, *J. Phys. Chem. C* **113**, 1662 (2009).

<sup>37</sup>M. Xu, J. Zhang, S. Wang, X. Guo, H. Xia, Y. Wang, S. Zhang, W. Huang, and S. Wu, *Sens. Actuators B* **146**, 8 (2010).

<sup>38</sup>F. Kong, Y. Wang, J. Zhnag, H. Xia, B. Zhu, Y. Wang, S. Wang, and S. Wu, *Mater. Sci. Eng. B* **150**, 6 (2008).

<sup>39</sup>Z. Jiao, G. Ye, F. Chen, M. Li, and J. Liu, *Sensors* **2**, 71 (2002).

<sup>40</sup>R. B. Waghulade, R. Pasricha, and P. P. Patil, *Talanta* **72**, 594 (2007).

<sup>41</sup>R. R. Salunkhe, D. S. Dhawale, U. M. Patil, and C. D. Lokhande, *Sens. Actuators B* **136**, 39 (2009).

<sup>42</sup>P. P. Sahay and R. K. Nath, *Sens. Actuators B* **133**, 222 (2008).

<sup>43</sup>G. N. Chaudhari, D. R. Bambole, and A. B. Bodade, *Vacuum* **81**, 251 (2006).